Program Digest, 2019 IEEE International Ultrasonics Symposium (IUS)
Glasgow, Scotland, October 6-9, 2019

Wavefield focusing with reduced cranial invasiveness

1st Giovanni Angelo Meles
Faculty of Civil Engineering & Geosciences
Delft University of Technology
Delft, The Netherlands
G.A.Meles@tudelft.nl

2nd Joost van der Neut
Faculty of Applied Sciences
Delft University of Technology
Delft, The Netherlands
J.R.vanderNeut@tudelft.nl

3rd Koen W. A. van Dongen
Faculty of Applied Sciences
Delft University of Technology
Delft, The Netherlands
K.W.A.vanDongen@tudelft.nl

4th Kees Wapenaar
Faculty of Civil Engineering & Geosciences
Delft University of Technology
Delft, The Netherlands
C.P.A.Wapenaar@tudelft.nl

***Abstract*—Wavefield focusing can be achieved by Time-Reversal Mirrors, which involve in- and output signals that are infinite in time and waves propagating through the entire medium. Here, an alternative solution for wavefield focusing is presented. This solution is based on a new integral representation where in- and output signals are finite in time, and where the energy of the waves propagating in the layer embedding the focal point is reduced. We explore the potential of the proposed method with numerical experiments involving a 1D example and a cranium model consisting of a skull enclosing a brain.**

***Index Terms*—utrasound, focusing, brain, invasiveness, Marchenko**

I. Introduction

Wavefield focusing can be achieved by Time-Reversal Mirrors (TRM) [1]. Theoretically, to achieve proper focusing, wavefields emitted by a source at the focal point are first evaluated at a boundary enclosing that focal point. Next, the wavefields are reversed in time and sent back into the medium. Unfortunately in TRM the resulting wavefields are infinite in time and propagate through the entire medium (Fig. 1a). Recently, it was shown that wavefields can also be focused from a single open-boundary with so-called Marchenko focusing functions, which are defined as the inverse of the transmission response in an auxiliary reference medium (defined to be identical to the actual medium *above* or *below* the focusing level and reflection-free *below* or *above* this depth level depending on whether focusing is sought from *above* or *below*, respectively). Crucially, focusing functions can be estimated by solving the Marchenko equation [2], [3], which does not require exact knowledge of any transmission response. When a Marchenko focusing function (in the following indicated as $f_1(t)$ and $f_2(t)$ if injected from *above* or *below*, respectively) is emitted in the auxiliary truncated medium, a peculiar focusing condition is achieved (Fig. 1b). When the solution of the Marchenko equation is emitted into the actual medium, a focus emerges at the focal point, followed by a causal Green's function that propagates through the entire medium [4]. Although the focusing function is finite in time, the Green's function emerging after wavefield focusing has infinite duration (Fig. 1c). In this paper, it will be discussed how to craft a focusing wavefield that, once injected in the medium from two open-boundaries, propagates to a specified focal point in finite time, without being followed by any Green's function (Fig. 1d). It will also be discussed how this focusing method theoretically reduces wavefield propagation in the layer which embeds the focal point. Numerical tests involving a complex model will show that wavefield propagation is largely reduced in the layer embedding the focal point despite the fact that exact focusing functions cannot be retrieved.

II. Methods

To overcome the problems associated with TRM we propose a Finite Time Focusing (FTF) method where the wavefields are focused using Marchenko functions. In FTF, series of wavefronts are emitted into the medium from the surrounding boundary in such a way that only the first wavefronts reaches the focal point [5]. The focusing performances of Marchenko functions and FTF are shown in an illustrative 1D scenario in Fig. 1. Note that, for this example, focusing functions are computed inverting the corresponding transmission responses.

When $f_1(t)$ is injected from above in the actual medium, focusing is not achieved if interfaces are located below the focusing point. This is shown in Fig. 1c, where green arrows point at scattering events due to reflectors (green dots) situated below the focusing point. However, these scattering events are suppressed in FTF by destructive interference with waves associated with propagation of $f_2(-t)$ from below (see black and red arrows in Fig. 1d). Analogous destructive interferences apply also to wavefields associated with injection of $f_2(t)$ from below and $f_1(-t)$ from above (compare dark and light blue and green dots in Fig. 1d). Therefore, in contrast to TRM, Marchenko focusing functions are confined in time and space by the direct propagation path from the boundary to the focal

978-1-7281-4595-2/19/$31.00 ©2019 IEEE

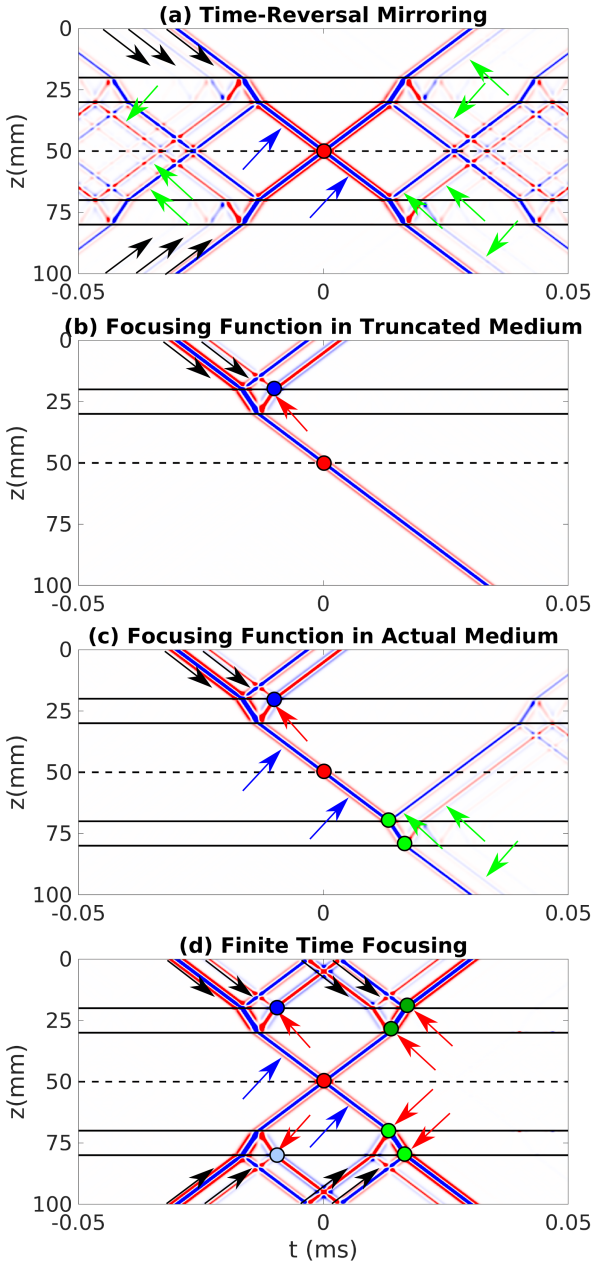

Fig. 1. (a) 1D TRM wavefield. The wavefield focuses at time $t = 0$ (red dot) and propagates through the entire medium indefinitely before and after time $t = 0$. Blue and green arrows indicate illustrative direct and scattered components of the wavefield, respectively, while black arrows represent actually injected wavefields. Solid and dashed lines stand for interfaces and the focusing depth. (b and c) 1D wavefields associated with injection from a single open-boundary (defined at $z = 0$) of $f_1(t)$ in the (b) truncated and (c) actual medium. Black arrows indicate wavefields injected at the surface interfering destructively at an interface (blue dot) with scattered events (red arrows), resulting in focusing at time t=0 at the focal point in the truncated medium. Green arrows in (c) indicate scattering events due to interfaces (green dots) situated below the focusing point interfering with the focal point. (d) 1D FTF, involving injection from two open-boundaries (defined at $z = 0$ and $z = 100$ mm, respectively) of the superposition of $f(t)$ and $f(-t)$ (see Eq. 1). As in (c), black and red arrows indicate events interfering destructively at interfaces situated above and below the focusing point (dark and light blue and green dots, respectively). Cancellation of Green's function scattering terms results in focusing at time t=0 at the focal point in the actual medium. The wavefield is then confined within a spatial-temporal window defined by the propagation of the initial component of the focusing function.

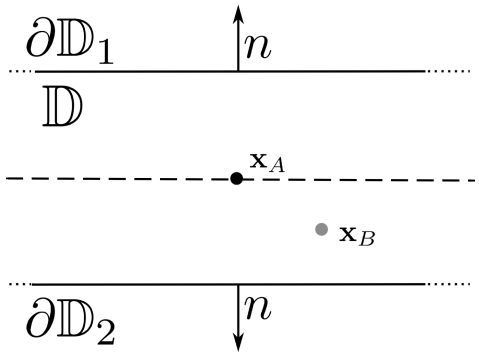

Fig. 2. (c) Cross-section of the configuration for Eq. (1) Volume $\mathbb{D}$ is surrounded by $\partial\mathbb{D}_1$ and $\partial\mathbb{D}_2$ with outward-pointing normal vectors n. The focal point is at $\mathbf{x_A}$ along the focal plane (dashed line), while $\mathbf{x_B}$ represents any point inside volume $\mathbb{D}$.

point [2]. This is mathematically expressed in the frequency domain (for a complete derivation see [6]) by:

$$\begin{aligned} &2\Re\{f(\mathbf{x}_B,\mathbf{x}_A;\omega)) \\ &= \int_{\partial\mathbb{D}_1\cup\mathbb{D}_2} d^2\mathbf{x}\frac{1}{j\omega\rho(\mathbf{x})}(G(\mathbf{x},\mathbf{x}_B,\omega)n_3\partial_3 2\Re(f(\mathbf{x},\mathbf{x}_A,\omega)) \\ &\quad -2\Re(f(\mathbf{x},\mathbf{x}_A,\omega))n_3\partial_3 G(\mathbf{x},\mathbf{x}_B,\omega)), \end{aligned} \tag{1}$$

where

$$\begin{aligned} &f\left(\mathbf{x},\mathbf{x}_A;\omega\right) = \\ &\theta\left(\mathbf{x}_{3,A}-\mathbf{x}_3\right) f_1\left(\mathbf{x},\mathbf{x}_A;\omega\right) + \theta\left(\mathbf{x}_3-\mathbf{x}_{3,A}\right) f_2\left(\mathbf{x},\mathbf{x}_A;\omega\right). \end{aligned} \tag{2}$$

Here $\partial\mathbb{D}_1$ and $\partial\mathbb{D}_2$ are horizontal boundaries enclosing the medium from above and below, respectively, $\mathbf{x}_A$ is the focal point and $\mathbf{x}_B$ is any point inside the domain $\mathbb{D}$, while θ is the Heaviside function indicating that $\theta\left(\mathbf{x}_{3,A}-\mathbf{x}_3\right) f_1\left(\mathbf{x},\mathbf{x}_A;\omega\right)$ and $\theta\left(\mathbf{x}_3-\mathbf{x}_{3,A}\right) f_2\left(\mathbf{x},\mathbf{x}_A;\omega\right)$ are non-zero only above and below the focal plane, respectively (see Fig. 2). The time-domain interpretation of Eq. 1 implies that by injecting into the medium the superposition of the causal $f(t)$ and the a-causal $f(-t)$ focusing functions, one can reconstruct this wavefield throughout the volume. Due to the intrinsic properties of focusing functions, i.e. the destructive interference of the codas with up- and down-going reflections, any scattering event is confined within a spatial-temporal window defined by the propagation of direct components of the focusing functions (for more details see [3], [6]). Finite Time Focusing is not limited to 1D media, and Fig. 3 shows an example of FTF for a 2D head model consisting of a skull enclosing a brain. In this case the focusing function $f_1(t)$ is estimated using a standard acquisition configuration rather than by inverting the corresponding transmission responses [3]. More precisely, iterative substitution of the coupled Marchenko equations allows to retrieve focusing functions associated with arbitrary locations in a medium. The methodology requires as input the single-sided reflection response at the acquisition surface and an estimate of the initial focusing function, i.e. the Time-Reversed direct wavefield from the specified location in the

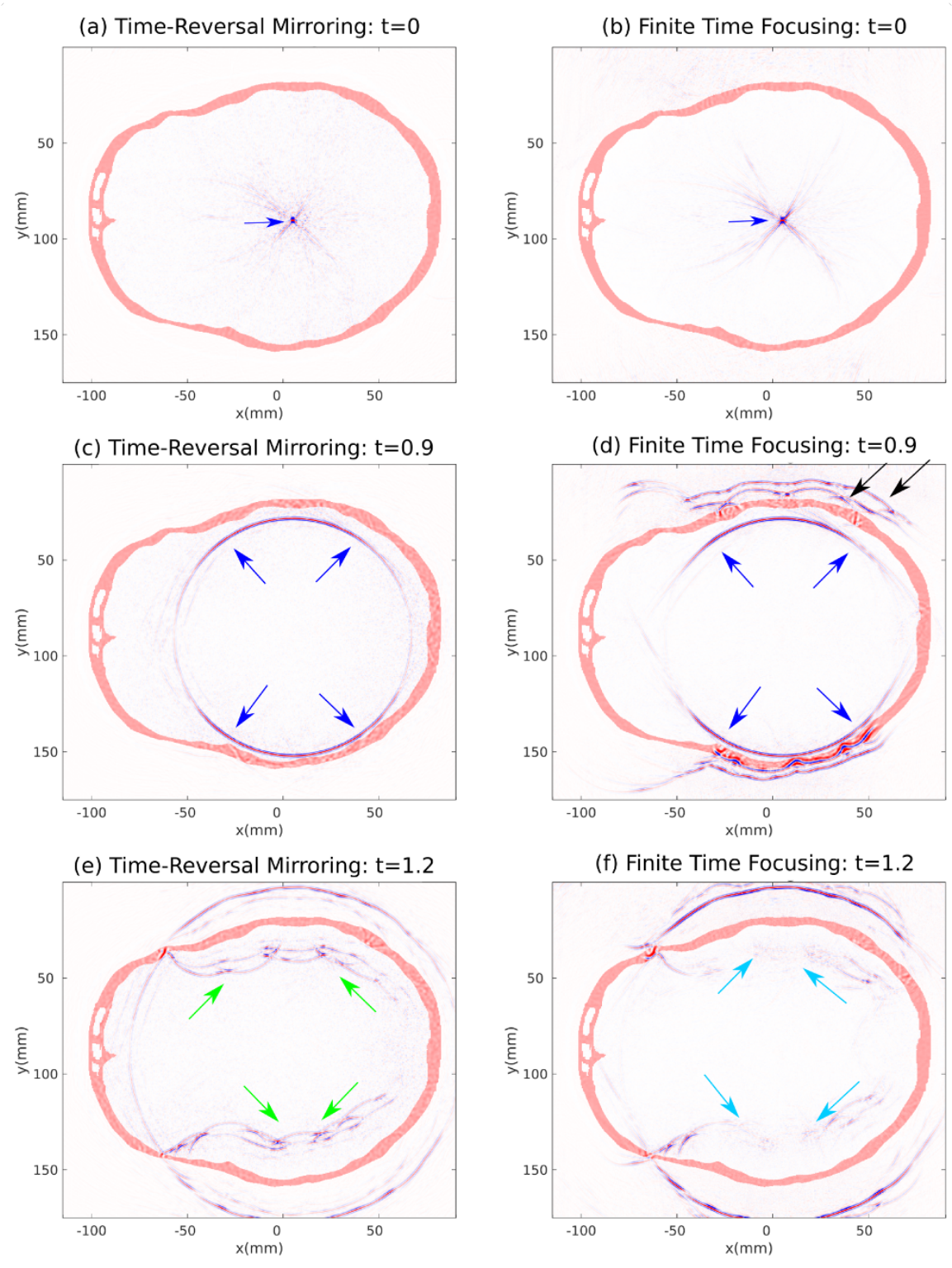

Fig. 3. Focusing properties of TRM and FTF solutions. Left column: Snapshots of the TRM solution when partial boundaries are considered. Due to the finite extent of the injection boundaries, small amplitude artefacts contaminate the wavefield at time $t = 0$, but good focusing is achieved (blue arrow in (a)). At times $t > 0$ the wavefield is seen propagating inside the skull (blue arrows in (c) indicate the direct wavefronts) until it gets reflected by the skull (green arrows in (e) point at strong scattering events being sent back into the skull). Right column: Snapshots of the FTF solution. A focusing comparable to what is provided by TRM is achieved at time $t = 0$ (blue arrow in (b)). As for the TRM case, at times $t > 0$ the wavefield is also seen propagating inside the skull (blue arrows in (d) indicate the direct wavefronts). However, in the meantime the coda of the focusing function is approaching the skull (black arrows in (d)). As the wavefield emanating from the focal point reaches the skull, it destructively interferes with the coda of the focusing function, resulting in reduced amplitude reflections (compare the wavefronts indicated by green and light blue arrows in (e) and (f), respectively).

subsurface to the acquisition surface. Here, to retrieve the focusing function $f_1(t)$, reflection data are then collected along the *upper* boundary of the model ($y = 0$ in Fig. 3), while the initial focusing function with a $0.8MHz$ Ricker wavelet emanating from the focal point (indicated by the blue arrow in in Fig. 3a,b) is computed in the actual skull model. Similarly, the focusing function $f_2(t)$ is estimated using reflection data collected along the *lower* boundary of the model ($y = 1750$ mm in Fig. 3).

III. Discussion

The wavefields resulting from TRM have infinite support in time, which could be inadvisable for various applications. Things are different in FTF (Eq. (1)), which involves wavefields that are bounded in time and space by the direct propagation path from the boundary to the focal point. As can be observed in Figs. 1, and 3, the superposition of $f(t)$ and $f(-t)$ contains a series of events that once emitted into the medium from the surrounding boundary interfere destructively with any ingoing reflection of the direct wavefield. Even when perfect focusing is not achieved, the amplitude of ingoing reflected waves is at least suppressed. Hence, the focusing function might be an attractive solution of the wave equation for focusing beyond strong acoustic contrasts. Here, by canceling or reducing the amplitude of ingoing reflections, from the skull we achieve the ideal situation of a single wavefront or reduced energy to reach the focal point and propagate along the focal plane. The peculiar nature of the focusing achieved by Eq. (1) therefore minimizes the spatial exposure to the incident wavefield of the layer embedding the focal point (see Fig. 4), and this could possibly be beneficial for sensitivity analysis and/or safety concern in medical treatment [7].

IV. Conclusions

A new strategy for wavefield focusing in an acoustic medium has been discussed. Unlike in standard Time-Reversed acoustics, the input and output signals for this type of focusing are finite in time and only involve propagation of direct waves in the layer that embeds the focal point. This leads to a reduction of spatial and temporal exposure when wavefield focusing is applied in practice. The method has been validated numerically for a head model consisting of hard (skull) and soft (brain) tissue. There results confirm that the proposed method can outperform classical Time-Reversed acoustics.

Acknowledgment

This research has been partly funded by the European Research Council (ERC) under the European Union's Horizon 2020 research and innovation programme (grant agreement No: 742703). Joost van der Neut is grateful to Niels Grobbe (University of Hawaii) for stimulating discussions and collaboration in the initial research that evolved into this contribution.

References

[1] M. Fink, Journal of Physics D: Applied Physics, *Time-reversal mirrors*, **26**, 1333-1350 (1993).
[2] J. H. Rose, Inverse Problems, *Single-sided autofocusing of sound in layered media*, **18**, 1923-1934 (2002).
[3] K. Wapenaar, J. Thorbecke, J. Van Der Neut, F. Broggini, E. Slob, and R. Snieder, Geophysics, *Marchenko imaging*, *79*, WA39WA57 (2014).
[4] K. Wapenaar, and J. Thorbecke, Geophysical Prospecting, *Virtual sources and their responses, Part I: time-reversal acoustics and seismic interferometry*, **65**, 1411-1429 (2017).
[5] F. Broggini and R. Snieder, European Journal of Physics, *Connection of scattering principles: A visual and mathematical tour*, **33**, 593-613 (2012).
[6] G.A. Meles, J. van der Neut, K. W.A. van Dongen, and K. Wapenaar, The Journal of the Acoustical Society of America, *Wavefield finite time focusing with reduced spatial exposure*, *145*(6), 35213530 (2019).
[7] A. Hughes, K. Hynynen, Physics in Medicine & Biology, *Design of patient-specific focused ultrasound arrays for non-invasive brain therapy with increased trans-skull transmission and steering range*, **17**, L9-L19 (2017).

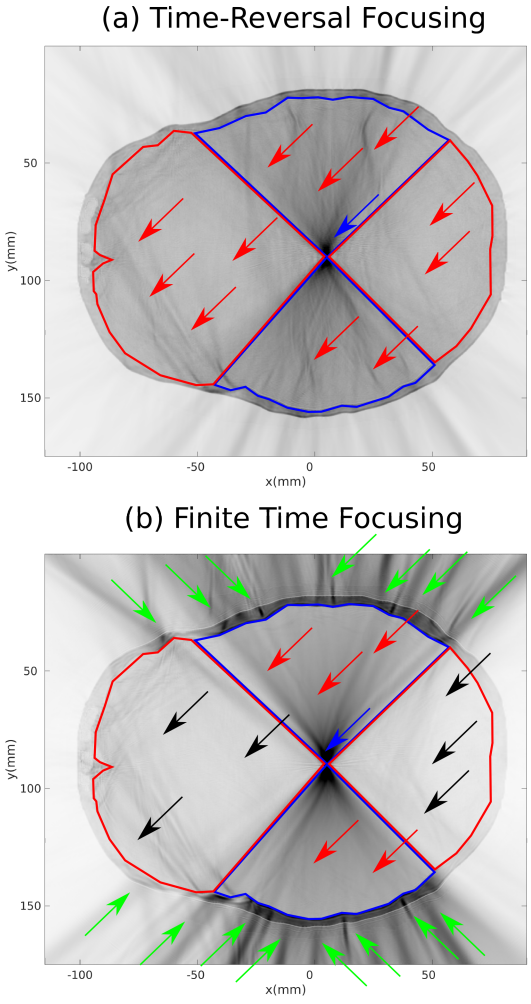

Fig. 4. Normalized L_2 norm of the pressure wavefields associated with TRM (a) and FTF (b). In Standard TRM (a), the norm of the pressure wavefield exhibits a peak at the focal point (blue arrow in a), and significant values are almost In FTF, the wavefield is still exhibiting a peak at the focal point (blue arrow in (b)) but it is somehow confined into a double cone centered at the focal point (blue cones in (b)). Black and green arrows point at regions of the brain with minimal wavefield invasiveness and large amplitude associated with the propagation of the coda of the focusing functions, respectively.